Energy barriers and chemical properties in the coadsorption of carbon monoxide and oxygen on Ru(0001)

Catherine Stampfl[1,2] and Matthias Scheffler[2]
[1]*Department of Physics and Astronomy, Northwestern University, Evanston 60208-3112, Illinois*
[2]*Fritz-Haber-Institut der Max-Planck-Gesellschaft, Faradayweg 4-6, D-14195 Berlin-Dahlem, Germany*
(Received 24 September 2001; published 3 April 2002)

Using density-functional theory we investigate the interactions and chemical properties of the coadsorption of carbon monoxide and oxygen on ruthenium (0001). For the adsorption phases that occur in nature, where CO occupies the top site, we find that with increasing oxygen coverage, the adsorption energy of CO can remain practically unchanged or even exhibit a slight *increase*. We attribute the increase to an O-induced lateral weakening of Ru-Ru bonds of non-O-bonded surface Ru atoms. Thus, these non-O-bonded Ru atoms can form stronger bonds to an on-top CO adsorbate. In contrast, a more expected behavior of a notable decrease in CO adsorption energy with increasing O coverage is observed only if the O atoms bond to the *same* Ru atoms as CO as, for example, is the case when CO occupies hollow sites. Furthermore, for some of the structures, we find that there is a manifestation of small activation energy barriers for CO adsorption well above the surface.

DOI: 10.1103/PhysRevB.65.155417 PACS number(s): 68.43.Bc

I. INTRODUCTION

Understanding the interactions and behavior of the coadsorption of different atomic and molecular species at surfaces is of considerable importance for many technological processes, for example, heterogeneous catalysis, corrosion, and gas sensors;[1–6] yet, on a microscopic level, such knowledge is still rather limited. Adparticles on metal surfaces can interact with each other directly, e.g., through induced dipole moments or wave function overlap, or via ''through-substrate'' interactions mediated by the substrate surface band structure (see, e.g., Ref. 7); they may also significantly affect the physical properties and chemical activity of neighboring atoms. The latter effect is, for example, exploited in the deliberate introduction of so-called ''promoter'' species to the surface to enhance the reactivity and control the selectivity of a catalyst, and is also noticeable when there are ''poisoner'' species present which adversely affect the reaction; usually reducing or quenching the reaction rate.

In the present work we study, through density-functional theory (DFT) calculations, the coadsorption of carbon monoxide and oxygen on ruthenium. The coadsorption of these species on transition metal surfaces is of particular relevance to various heterogeneous catalytic reactions, for example, carbon monoxide oxidation (see, e.g., Refs. 1 and 8–14). With respect to the adsorption of oxygen on Ru(0001), studies have shown that a full monolayer coverage (1×1)-O structure can form when high O_2 pressures are used or a highly oxidative molecular species such as NO_2 is employed at elevated temperatures ($\approx$600 K).[15,16] This is in contrast to earlier studies performed under ultrahigh-vacuum (UHV) conditions where the maximum coverage is found to be about 0.6 monolayers. This apparent saturation coverage is due to activation barriers for O_2 dissociation that build up due to the adsorbed O. The high-coverage (1×1)-O structure has been shown to be not very reactive towards CO_2 formation.[11,17] However, surfaces with much higher oxygen loadings can be formed depending on the temperature and pressure, and these exhibit a significantly enhanced reactivity for CO_2 formation.[12,13] The high reactivity has been linked to the formation of RuO_2 oxide crystallites on the Ru(0001) surface.[14] Recent theoretical investigations into the adsorption of O in excess of one monolayer at the Ru(0001) surface,[18–20] as well as the atomistic mechanism by which RuO_2 oxide might form, have been carried out.[19,20] These studies predict that oxygen in the subsurface region prefers to stay close to the surface and to give rise to island formation. The local atomic geometry in the islands can be described as a trilayer structure, and it is suggested that this represents a precursor (and nucleation) phase to the oxide formation. It has been pointed out[21] that with respect to oxidation catalysts, it may in fact be more common than hitherto expected that the initially introduced metal does not just adsorb oxygen, but that the catalytically active material contains subsurface oxygen as well as surface-oxide phases, some of which may even be unknown at present, as they may not exist under UHV conditions.

As is evident from above, the interaction of O with Ru(0001) is complex and depends sensitively on the gas phase pressure and temperature. Before attempting to investigate the interaction of CO and O on these more complex structures involving surface oxides and/or subsurface oxygen, it is first important to understand the behavior of coadsorbed CO and O on a clean Ru(0001) surface. The O,CO/Ru (0001) system represents an ideal model coadsorption system for fundamental study since it is very well characterized experimentally and the known periodic structures that form have the same surface unit cell; i.e., (2×2)-$(1O_h+1CO_t)$ (Refs. 9, 22, and 23), (2×2)-$(2O_{h,f}+1CO_t)$ (Ref. 24), and (2×2)-$(1O_h+2CO_{t,f})$ (Ref. 25) phases have been identified. [The top, hcp, fcc, and bridge sites are indicated by the subscripts t, h, f, and b, respectively, and in the case where two subscripts are given—e.g., ''$2O_{h,f}$''—it means that there are two of these particles in the surface unit cell, where one occupies the first site indicated and the other one occupies the second site indicated. Below we often omit

indicating the (2×2) periodicity each time since it is the same for all systems considered.] In an earlier publication[26] we compared the atomic geometry of these structures as obtained by low-energy electron diffraction (LEED) intensity analyses and by our DFT calculations, where very good agreement was found. We also proposed that a high-density (2×2)-($3O_h$+$1CO_h$) structure may represent a new stable phase, provided that kinetic barriers for adsorption could be overcome.

In this paper we focus on the energetics and chemical properties of the above-mentioned structures, as well as artificial CO,O coadsorption geometries. We identify various interesting mechanisms, which we expect will also be relevant for other similar systems: We find that for atomic configurations where CO occupies the top site, its adsorption energy can remain practically unchanged or even exhibit a slight *increase* with *increasing* O coverage, in contrast to a decrease as has been expected.[27,28] We propose that the slight increase of the CO adsorption energy with increasing O coverage found can be explained as being due to an O-induced reduction of the effective coordination of the non-O-bonded surface Ru atom to which CO is adsorbed. Behavior consistent with the more generally expected behavior of a notable *decrease* in the CO adsorption energy with *increasing* O coverage is observed when CO occupies a hollow site; the crucial factor dictating the affect on the CO adsorption energy is thus not the oxygen coverage *per se*, but rather the number of O bonds to the *same* metal atom that CO bonds to. For increasing numbers of such O-Ru bonds, the CO adsorption energy is significantly and sequentially decreased. Finally, on investigating the energetics of CO *above* the surface, we find for certain phases the presence of activation barriers to adsorption which are preceded by a weak physisorption well. Such barriers may be expected for *dissociative* molecular adsorption, where breaking of bonds occurs and new bonds are formed. However, for nondissociative adsorption of CO (and other small molecules) such barriers are not typically expected.

II. CALCULATION METHOD AND DEFINITIONS

Our DFT calculations are performed using the pseudopotential[29,30] plane-wave[31] method with the generalized gradient approximation (GGA) for the exchange-correlation functional[32] and the supercell approach to model the surface structures which are created on one side of a four-layer metal slab. The energy cutoff is 40 Ry and calculations were performed using three[33] and thirty[34] **k** points in the irreducible part of the Brillouin zone of the (1×1) surface unit cell. The smaller set is used to test the convergence of the calculations with respect to the **k**-point sampling and to investigate the phase space for possible activation energy barriers for CO above the surface. Calculations are then performed around identified barrier maxima and physisorption minima with the larger set. The associated energy differences are found, however, to be no more than 0.025 eV. Also, for the adsorption structures, results for the two different **k** points deviate at most for the adsorption energy, work-function change, and bond length by just 0.05 eV, 0.06 eV, and 0.03 Å, respectively. Test calculations for thicker layer slabs—namely, six layers—show that the adsorption energies differed by only 0.04 eV. The vacuum region is taken to be equivalent to nine bulk layers (≈20 Å) and the atomic positions of all atoms are relaxed except for the bottom two Ru layers which are held fixed at their bulklike positions. For further details we refer to Refs. 15 and 26. In the following sections we analyze our results through the calculation of various properties which are defined below.

The adsorption energy per adparticle is calculated as the difference of the total energy of the adsorbate-substrate system and the total energy of the clean (or reference) system together with that of the corresponding number of free adparticles. For example, the adsorption energy of a CO molecule on the Ru(0001) surface with n adsorbed O atoms per (2×2) cell is given by

$$E_{\mathrm{ad}}^{\mathrm{CO}/n\mathrm{O}-\mathrm{Ru}} = -E^{(n\mathrm{O}+\mathrm{CO})/\mathrm{Ru}} + E^{n\mathrm{O}/\mathrm{Ru}} + E^{\mathrm{CO}}, \tag{1}$$

where $E^{(n\mathrm{O}+\mathrm{CO})/\mathrm{Ru}}$ is the total energy of the adsorbate system, $E^{n\mathrm{O}/\mathrm{Ru}}$ is the total energy of the Ru(0001) substrate with n adsorbed O atoms, and E^{CO} is the total energy of a free CO molecule.

The difference electron density is defined as

$$n^{\Delta}(\mathbf{r}) = n(\mathbf{r})^{(n\mathrm{O}+\mathrm{CO})/\mathrm{Ru}} - n(\mathbf{r})^{n\mathrm{O}/\mathrm{Ru}} - n(\mathbf{r})^{\mathrm{CO}}, \tag{2}$$

where $n(\mathbf{r})^{(n\mathrm{O}+\mathrm{CO})/\mathrm{Ru}}$ is the total valence electron density of the coadsorption system, $n(\mathbf{r})^{n\mathrm{O}/\mathrm{Ru}}$ is that of the corresponding nO/Ru(0001) adsorbate structure, and $n(\mathbf{r})^{\mathrm{CO}}$ that of the free CO molecule. In Eq. (2), $n(\mathbf{r})^{(n\mathrm{O}+\mathrm{CO})/\mathrm{Ru}}$ is evaluated at the fully relaxed atomic positions and $n(\mathbf{r})^{n\mathrm{O}/\mathrm{Ru}}$ is obtained at these same atomic positions, but without the presence of the CO molecule. The total valence electron density is calculated as

$$n(\mathbf{r}) = \int_{-\infty}^{\infty} f(\epsilon, T) n(\mathbf{r}, \epsilon) d\epsilon = \sum_{i=1}^{\infty} f(\epsilon_i, T_{\mathrm{el}}) |\varphi_i(\mathbf{r})|^2, \tag{3}$$

where $f(\epsilon, T)$ is the Fermi distribution at temperature T, and $\varphi_i(\mathbf{r})$ are the single-particle eigenfunctions of the Kohn-Sham Hamiltonian. The local density of states (DOS) is

$$n(\mathbf{r}, \epsilon) = \sum_{i=1}^{\infty} |\varphi_i(\mathbf{r})|^2 \delta(\epsilon - \epsilon_i), \tag{4}$$

and the state-resolved DOS, or projected DOS, is given by

$$N_{\alpha}(\epsilon) = \sum_{i=1}^{\infty} |\langle \phi_{\alpha}(\mathbf{r}) | \varphi_i(\mathbf{r}) \rangle|^2 \delta(\epsilon - \epsilon_i), \tag{5}$$

where $\phi_{\alpha}(\mathbf{r})$ is a properly chosen localized function. For $\phi_{\alpha}(\mathbf{r})$ we use the eigenfunctions of the isolated pseudoatoms, which are truncated at a radius of 2.0 bohrs.

III. DEPENDENCE OF CO ADSORPTION ENERGY ON O COVERAGE

A. CO constrained in the hcp hollow site

We first discuss the adsorption energy of CO on a clean Ru(0001) surface for the various sites. The energy difference

TABLE I. Adsorption energy of CO, E_{ad}; work-function change $\Delta\Phi$; and bond length between Ru and C, $b_{Ru\text{-}CO}$, and between C and O, $b_{C\text{-}O}$. The calculated work function of the clean surface is 5.08 eV. The numbers (0), (1), and (2), indicate the C-Ru bonds that have zero, one, and two O atoms bonded to the Ru atom. Also convergence checks for two different **k**-point sets are listed. The deviations in the quantities are given as δ. The subscripts "h,f" on "2O" indicate that one of the O atoms in the surface unit cell occupies the hcp-hollow site and that the second one occupies the fcc-hollow site. Similarly for the subscripts "t,f" on "2CO," this indicates that one of the CO molecules occupies the top site and the second one in the surface unit cell occupies the fcc-hollow site. The "b" refers to the bridge site.

Structure	E_{ad} (eV)			$\Delta\Phi$(eV)			$b_{Ru\text{-}CO}$ (Å)			$b_{C\text{-}O}$ (Å)		
	3 kpt	30 kpt	δE_{ad}	3 kpt	30 kpt	$\delta\Phi$	3 kpt	30 kpt	$\delta b_{Ru\text{-}CO}$	3 kpt	30 kpt	$\delta b_{C\text{-}O}$
(2×2)-CO_b	–	1.58	–	–	0.90	–	–	2.11	–	–	1.19	–
(2×2)-CO_f	–	1.61	–	–	0.88	–	–	2.18	–	–	1.19	–
(2×2)-CO_h	–	1.70	–	–	0.97	–	–	2.18	–	–	1.20	–
(2×2)-CO_t	–	1.79	–	–	0.51	–	–	1.92	–	–	1.17	–
$1O_h+1CO_t$	1.68	1.72	0.04	0.75	0.75	0.00	1.95	1.94	−0.01	1.16	1.16	0.00
$2O_{h,f}+1CO_t$	1.80	1.77	−0.03	1.22	1.21	−0.01	1.92	1.95	0.03		1.16	0.00
$(1O_h+2CO_{t,f})$:CO_t	–	1.66	–	1.10	1.16	0.06	1.97	1.96	−0.01	1.16	1.16	0.00
$(1O_h+2CO_{t,f})$:CO_f	1.28	1.23	−0.05	"	"	"	2.24	2.21	−0.03	1.19	1.19	0.00
$1O_h+1CO_h$	1.30	–	–	1.29	–	–	2.13(1), 2.21(0)	–	–	1.19	–	–
$2O_h+1CO_h$	1.03	–	–	1.57	–	–	2.14(2), 2.16(1)	–	–	1.19	–	–
$3O_h+1CO_h$	0.85	0.84	−0.01	1.73	1.69	−0.04	2.14	2.17	0.03	1.18	1.18	0.00

between adsorption of CO in the hcp hollow site and in the on-top site is calculated to be 0.09 eV, where the on-top site is energetically more favorable. The fcc site for CO is 0.09 eV less favorable than the hcp site, thus 0.18 eV less favorable compared to the on-top site, and the bridge site for CO adsorption is 0.21 eV less than for CO in the on-top site. These values are listed in Table I, along with the associated work-function change, CO bond lengths and C-Ru distances. We note that CO adsorption on Ru (0001) for coverages $\Theta_{CO}\leqslant 1/3$ ML actually forms islands with a $(\sqrt{3}\times\sqrt{3})R30°$ structure[35] where CO assumes the on-top site,[36,37] but it is more instructive in the present work to use the (2×2) surface cell, since then any observed changes with increasing O coverage can be identified as being just due to the adsorbed O atoms and not due to the surface periodicity or coverage.

We note in passing that the local-density approximation (LDA) and Perdew-type GGA's tend to favor structures with higher coordination, and for some systems the calculated CO adsorption site appears to be incorrect.[38] The reason for the high-coordination preference is believed to be that the LDA and, also, Perdew-type GGA's are "jellium derived" and therefore prefer a more delocalized, more metalliclike bonding. Apparently, for Ru, which forms stronger covalent bonds than the very late transition and noble metals (e.g., Pt), this problem is not significant.

In the following we investigate the change in the adsorption energy of CO with increasing O coverage. Specifically, we place CO in the *hcp hollow* site and consider increasing concentrations of O in neighboring hcp sites. As a reference energy we use the adsorption energy of CO on the bare surface (no oxygen present) with a (2×2) periodicity in the hcp site. As indicated earlier, CO actually assumes on-top sites in the *stable* coadsorption structures identified to date[23–25] and in the pure CO adsorption system (see above). It is nevertheless informative to study these more "academic structures" in order to improve our understanding of the generic behavior of these (and similar) coadsorption systems. Actually, depending on the experimental preparation of the CO,O/Ru (0001) systems, CO may in fact occupy such hollow sites (or near hollow sites) in the coadsorption with oxygen, existing as a *metastable* phase, i.e., adsorption of CO at *low* temperature on the (2×1)-O phase—only on annealing or adsorption at elevated temperatures (300 K) does the $2O_{h,f}+1CO_t$ phase result with CO in the on-top site.[24]

The results for the adsorption energy of CO in the hcp site on Ru(0001) with increasing O coverage are shown in Fig. 1 (left) where diagrams of the corresponding surface structures are also included. It can be seen that there is a strong decrease in the CO adsorption energy with increasing O coverage; for the structure with six oxygen neighbors the decrease is a large 0.8 eV. We note that for the calculations with two and four O neighbors, we had to fix the lateral position of the

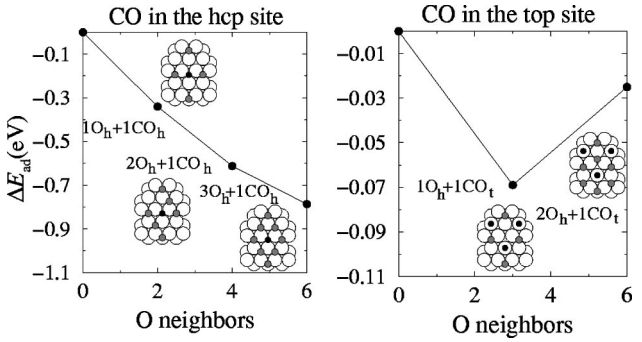

FIG. 1. Adsorption energy of CO in the hcp site (left) and of CO in the on-top site (right) as a function of the number of O neighbors. Note the scale on the *y* axis on the left is a factor of 10 less than that of the right. In both figures, the first point, i.e., the energy zero, is for CO adsorption on the clean surface. Insets depict the corresponding surface structures: Large white, small black, and gray circles represent Ru, CO, and O, respectively.

CO molecule during the atomic relaxation, since if we did not, CO moved towards the Ru atom(s) which has the least number of O atoms bonded to it; i.e., for the $1O_h+1CO_h$ structure, CO is attracted to the single Ru atom in the surface unit cell that is not bonded to oxygen, and for the $2O_h+1CO_h$ structure [where the O atoms are arranged in a (2×1) geometry], CO moves towards the two Ru atoms (i.e., the bridge site) that have one bond to an O atom, as opposed to the Ru atom in the unit cell that is bonded to two O atoms. Extending the curve of Fig. 1 (left) by placing an O atom directly below the CO molecule in the tetrahedral (tet) site between the first and second Ru layers, corresponding to a $4O_{3h,tet}+1CO_h$ coverage, the CO molecule is completely destabilized and leaves the surface. This behavior can be explained in that the presence of the electronegative coadsorbate, O, competes for metal electrons and reduces the charge transfer from the metal into the $2\pi^*$ CO orbital. Since the latter orbital is bonding for the CO-metal bond and antibonding for the C-O bond,[39] the former is expected to be weakened and the latter strengthened. Conversely, it is interesting to consider how the presence of adsorbed CO affects the O adsorption energy. For the O coverages of 0.25, 0.5, and 0.75 (Fig. 1, left), the O adsorption energies are reduced by 0.34, 0.30, and 0.26 eV per O atom, respectively. Thus, preadsorbed CO in the hcp site similarly weakens the O-Ru bond strength. That is, the valence electrons of the Ru atom which build bonds with the CO molecule and O atoms have to hop from Ru-CO bonds to Ru-O bonds and are therefore less efficient for the individual Ru-X bond strength (here X stands for either CO or O). We may state this in even more general terms: a covalent bond of an atom (or molecule) A with a transition metal atom, Ru in this case (A-Ru), is weakened if the transition metal is also bonded to another atom: A-Ru-B. We note that with increasing number of O bonds to surface Ru atoms, the Ru d band is sequentially broadened and its center shifted down in energy, and in this respect it is consistent with the picture that such a modified d band binds CO (and other adparticles) more weakly; see, e.g., Refs. 40 and 41.

From analysis of the projected density of states of the structures shown in Fig. 1 (left) and of the wave functions, we find that with increasing O coverage a hybridization of the CO 1π state, with states of the neighboring O atoms, occurs. This gives rise to lower- and higher-lying CO 1π-like states, where the CO 5σ-derived state is at an energy in between them. This is illustrated in Fig. 2 for the $3O_h+1CO_h$ structure which exhibits the largest effect. The CO 1π-related states lying on each side of the CO 5σ-like state can be clearly seen. Representative wave functions are shown as insets in Fig. 2 for two different cross sections. The lower-lying CO 1π-like state interacts with the O-$2p_{xy}$ orbitals of the neighboring O atoms (see upper, leftmost inset) exhibiting a bonding nature; the higher-lying feature has a less bonding and more antibondinglike character, as indicated by the different sign of the wave function at CO and the O atom (upper, rightmost inset). Occupation of these more antibondinglike states may contribute to the reduction in the adsorption energy. Furthermore, it can be seen that the surface Ru atoms are significantly involved in the formation

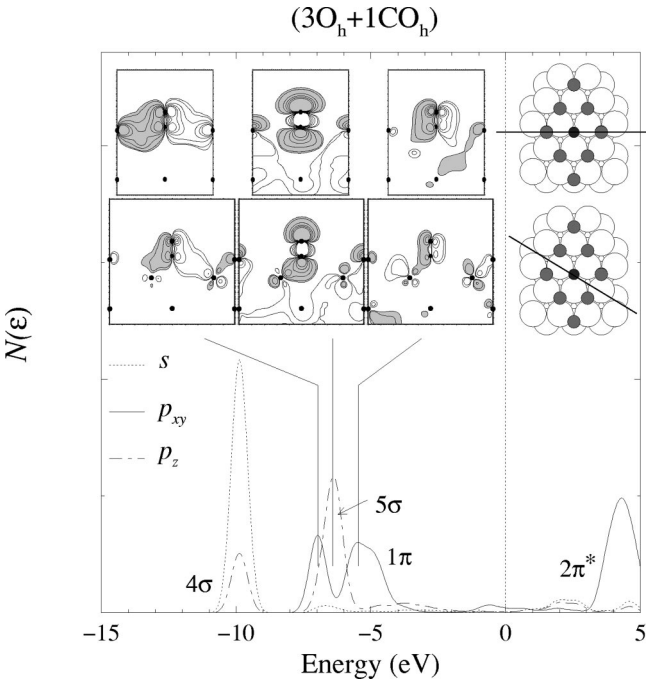

FIG. 2. Projected density of states on the C atom of the $3O_h+1CO_h$ structure, showing the hybridization of the CO-1π-like state with O-$2p_{xy}$-like states of neighboring O adatoms. Insets: representative wave functions, in the (1000) plane (upper) and the (1100) plane (lower) as indicated by the lines on the sketches of the atomic structure, for CO 1π-, 5σ-, and π-derived states at the respective energies of -7.01, -6.40, and -5.29 eV. The gray shaded and nonshaded regions correspond to different signs of the wavefunctions.

of these states (see lower insets of Fig. 2). From investigation of the mentioned CO-related states along the high-symmetry (Γ-M) line of the surface Brillouin zone, we find that these levels are very flat and exhibit only a small dispersion. The wave function for the CO 5σ-derived state is shown in the center panels.

It is interesting to consider how much less favorable these (artificial) structures, with CO in the hcp site, are as compared to the stable structures with CO in the top site: The total-energy difference between the $1O_h+1CO_h$ and $1O_h+1CO_t$ structures is 0.38 eV, and between the $2O_h+1CO_h$ and $2O_{f,h}+1CO_t$ structures, the value is 0.57 eV. The corresponding differences in the CO adsorption energies are 0.38 eV and 0.77 eV, respectively (see Table I). Note that the first numbers are the same in both cases (0.38 eV) which is due to the fact that the oxygen atoms are in the hcp sites for both structures and it is only the position of CO that is different. The second numbers differ because in the energetically preferred structure $2O_{f,h}+1CO_t$ there is one O atom in the hcp site and the other in the fcc site which is less favorable by 0.2 eV, as compared to when both O atoms are in the hcp site as is the case for $2O_h+1CO_h$. Thus the total-energy difference is 0.2 eV smaller than that of the adsorption-energy difference. The structures with CO in the top site are therefore significantly energetically more favorable and this is because CO can adsorb on non-O-bonded Ru atoms as will be seen and discussed below.

B. CO in the top site

We now turn to consider and compare the CO adsorption energy change with increasing O coverage for the case of CO in the on-top site, as occurs for the stable structures in nature and which are indeed the lower-energy structures in our DFT calculations. That is, now the positions of the adparticles are not fixed, but the particles assume the adsorption sites that yield the lowest total energy. The CO adsorption energies are shown in Fig. 1 (right), and the adsorption energies, work-function change, and CO bond lengths and distances between C and Ru are given in Table I. Interestingly, it can be seen that there is very little change in the CO adsorption energy with increasing O coverage; moreover, after a slight initial decrease (corresponding to the $1O_h+1CO_t$ structure), there is a slight *increase* in energy (of 0.05 eV) on going to the $2O_{h,f}+1CO_t$ phase, although this contains a *higher* O coverage. An important difference between the structures of Fig. 1, left versus right, is that in the former, CO bonds to Ru atoms, which also bond to O atoms, whereas in the latter, it does not. Thus, we see that in general, *a priori*, one should not necessarily expect a decrease in the CO adsorption energy with increasing O coverage; rather, one should expect a notable decrease with an increase in the *number of O atoms that bond to the Ru atoms to which CO is bound*. In relation to this, it can be said that the O-Ru and CO-Ru bonding is a rather localized (''nearsighted'') phenomenon since, although the O atoms are close neighbors, they affect the adsorption energy only modestly (and vice versa) and the main bonding of CO is to the single Ru atom below it. Concerning the initial slight decrease in adsorption energy in Fig. 1 (right) of CO for the $1O_h+1CO_t$ structure, the corresponding increase in the work function is 0.75 eV. This value is *less* than that of the sum of the separately adsorbed CO and O structures (2×2)-CO/Ru(0001) and (2×2)-O/Ru(0001), which are 0.51 eV and 0.35 eV, respectively, giving 0.86 eV. This indicates that in the coadsorption system there is an electrostatic (dipole-dipole) repulsion between the adsorbed CO and neighboring O adatoms, yielding a depolarization. We attribute this mechanism as being responsible for giving rise to the slight decrease in adsorption energy. This rather small decrease in adsorption energy is similar to that found for the (2×2)-$(1S_h+1CO_t)$/Rh(111) system studied in Ref. 42 in which CO also occupies the top site and S (which is below O in the periodic table and also electronegative) a hollow site.

With respect to the slight increase in adsorption energy with increasing O coverage (Fig. 1, right), i.e., on going from the $1O_h+1CO_t$ to $2O_{h,f}+1CO_t$ structures, from our analysis we propose that the increase is due to the following mechanism: Oxygen, adsorbed in the threefold hollow sites, forms strong bonds with the Ru atoms. The non-O-bonded Ru atom in the (2×2) unit cell thus loses bond strength with its six lateral Ru neighbors, which destabilizes this Ru atom. We verified this destabilization by calculating that the removal energy of this Ru atom [in the underlying (2×2)-$2O_{h,f}$ structure, i.e., without CO present] is significantly less than to remove a Ru atom from the clean surface; compare 0.27 eV to 1.70 eV. The removal energy for the non-O-bonded Ru atom in the (2×2)-O structure, with intermediate O coverage, is 1.06 eV, i.e., in between. We note that analogous calculations for O/Ag(111), where O occupies the fcc site, exhibit a similar effect where in this case the corresponding reduction is from 0.44 eV (of the clean surface) to just 0.12 eV of the (2×2)-O structure.[43] This weaker bonded surface Ru atom binds CO more strongly and we find that this gain in adsorption energy even overcompensates the electrostatic repulsion between CO and the adsorbed O atoms. This non-O-bonded surface Ru atom [of the (2×2)-$2O_{h,f}$ structure] has a slightly narrower and upshifted $4d$ band. These results reflect what we said above: This Ru is less strongly bonded to its Ru neighbors and is in line with the interpretation that such a change in the d band gives rise to stronger CO binding energies as has been found at step edges or on surfaces under tensile strain.[40] We note that recently an O-induced surface metal destabilization mechanism has been observed for O on Cr(100),[44,45] where in this case the bond weakening leads to the formation of a vacancy at the surface. We also investigated whether the presence of CO in the top site affects the adsorption energy of the O atoms: For the O coverages of 0.25 and 0.5 (Fig. 1, right) the average adsorption energy is found to decrease by 0.07 and 0.01 eV per O atom, respectively. Thus, CO has only a small influence as we may expect due to the above-mentioned localized nature of the CO bonding.

For comparison, we also carried out calculations for the corresponding structures but involving Na, which is electropositive on Ru, instead of O, which is electronegative. Interestingly, we find an *opposite* behavior: The removal energy of the non-Na-bonded Ru atom in the (2×2)-$1Na_f$ and (2×2)-$2Na_{h,f}$ structures *increases* with Na coverage, from 1.70 eV of the clean surface, to 1.73, to 1.87 eV. [Here in the (2×2)-Na_f structure, we place Na in the fcc site as occurs in nature.] In this case there is charge transfer from Na towards the surface, and the non-Na-bonded Ru atom becomes effectively higher coordinated and more stable, thus requiring more energy to remove it. Also, correspondingly, opposite to the case for CO in the top site on the O-precovered structures, CO in the top site on the (2×2)-$2Na_{h,f}$ structure yields an adsorption energy that is *weaker* than on the lower Na-coverage (2×2)-Na_f structure (by 0.2 eV), consistent with the notion of an *increased* stabilization of the non-Na-bonded Ru atom, and reduced reactivity towards adsorption of CO.

Coming back briefly to the differences in CO adsorption energy for adsorption in top and hollow sites, it can be seen from the values in Table I that the hollow site for CO adsorption is notably less favorable than the on-top site, i.e., by 0.56 eV for CO_f of the $1O_h+2CO_{t,f}$ structure and by 0.95 eV for the CO of the $3O_h+1CO_h$ structure (compared to top-site adsorption on the clean surface). This weaker adsorption energy is not due to just the adsorption site since for CO on the clean surface; the hcp–top-site energy difference is only 0.09 eV (see Table I). The main reason for the reduced adsorption energy (as discussed above) is due to the fact that in the fcc (hcp) site, CO bonds with three Ru atoms, each of which is also bonded to one (two) O atom(s) (see rightmost two atomic structures in the upper panel of Fig. 3). It is interest-

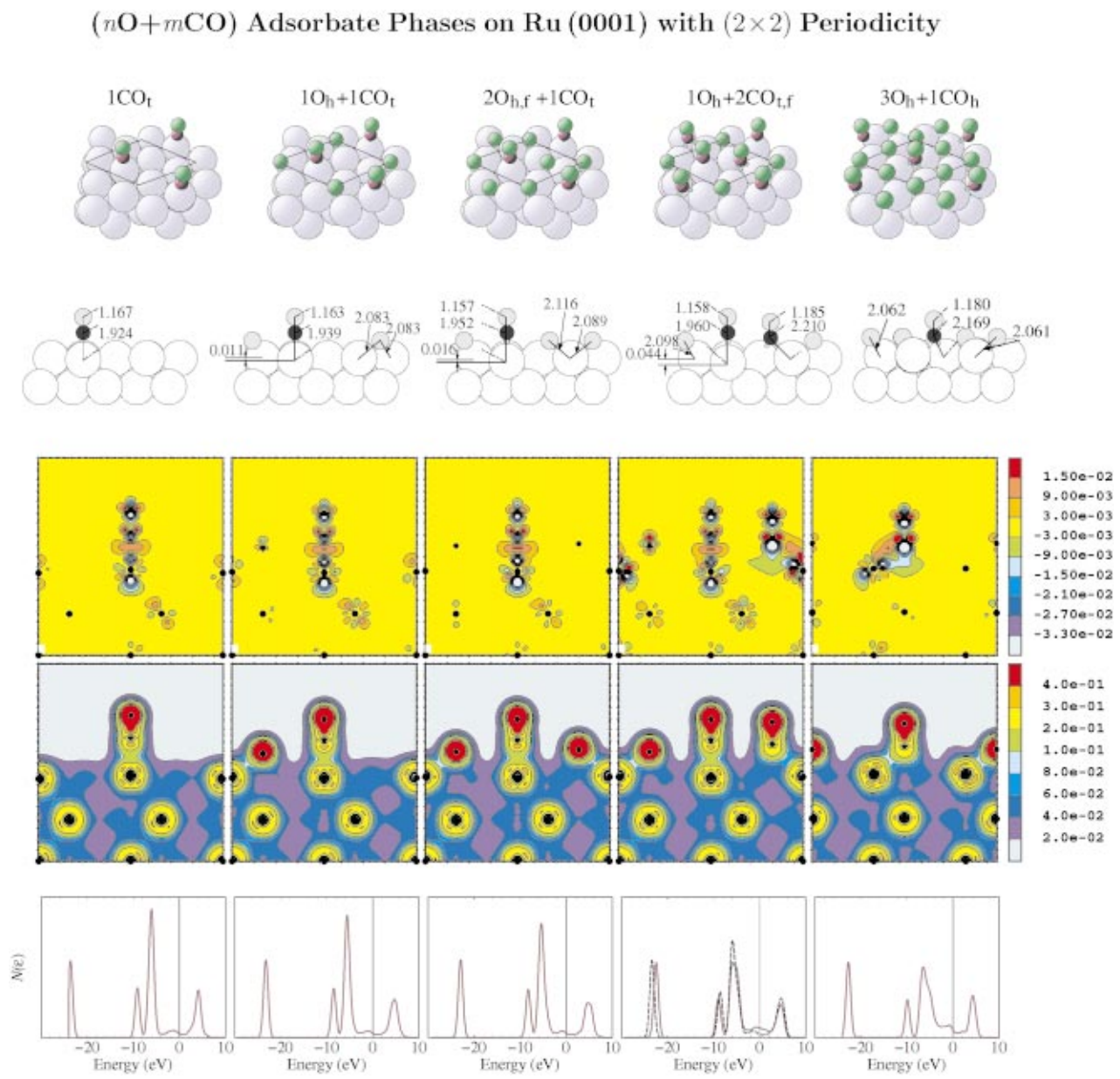

FIG. 3. (Color) Atomic structure (upper two panels), projected DOS (lower panel), and total electron density $n(\mathbf{r})$ (lower middle panel) and difference density $n^{\Delta}(\mathbf{r})$ (upper middle panel) distributions for the (2×2)-CO$_t$, 1O$_h$+1CO$_t$, 2O$_{h,f}$+1CO$_t$, 1O$_h$+2CO$_{t,f}$, and 3O$_h$ +1CO$_h$ structures (from left to right). The contour lines are given in bohr^{-3}. Large, small green, and small purple circles represent Ru, O, and C atoms, respectively. The dashed and solid lines in the density of states for 1O$_h$+2CO$_{t,f}$ correspond to the top and fcc sites, respectively.

ing to note that the value of the adsorption energy decrease of 0.47 eV (with respect to the adsorption energy of CO on the clean surface in the hcp site) for CO in the fcc site of the 1O$_h$+2CO$_{t,f}$ phase, in which it has three O neighbors, nicely fits the trend of a systematic and sequential decrease in CO adsorption energy with increasing O coverage, falling in between those having two and four O-Ru bonds (see Fig. 1, left), even though here the adsorption site is fcc as compared to hcp.

From the above discussions, we see that the adsorption energy of CO and, in this sense, its reactivity can be markedly changed by the presence of coadsorbates; the degree and sign of the change depending critically on the details of the *adsorption sites* involved, as well as on the species and coverage.

IV. ELECTRONIC STRUCTURE OF THE COADSORPTION SYSTEMS

The total valence electron density $n(\mathbf{r})$ [cf. Eq. (3)] and the difference density $n^{\Delta}(\mathbf{r})$ [cf. Eq. (2)] of the various phases are shown in Fig. 3, along with the sum of the DOS for projection on the atoms of the CO molecule. Of the molecular orbitals (MO's) of CO (1σ,2σ,3σ,4σ,1π,5σ,$2\pi^*$), the

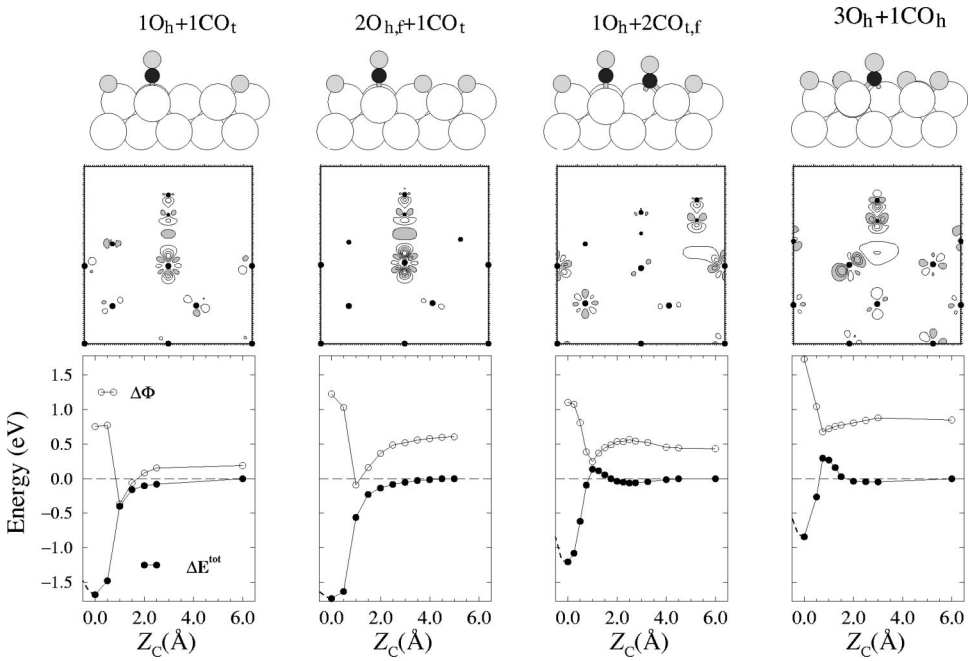

FIG. 4. Lower panels: change in work function (open circles) and total energy (solid circles) (referred to the situation where CO is far from the surface) as a function of distance of CO from its equilibrium position for $1O_h+1CO_t$, $2O_{h,f}+1CO_t$, $1O_h+2CO_{t,f}$ (for CO_f), and $3O_h+1CO_h$ as shown in the upper panels, from left to right. Middle panels: difference density distributions for CO at 1.0 Å above its equilibrium position on the surface. The contour lines are given in bohr^{-3} where the spacing is 0.003 with the first positive value (representing an increase of electron density shown as shaded) at 0.001 and the first negative contour line at −0.001.

two most important ones are the 5σ and $2\pi^*$ orbitals which correspond to the highest occupied MO (HOMO) and the lowest unoccupied MO (LUMO), respectively (see, e.g. Ref. 7). The notation here is that "σ" indicates orbitals that have electron density that is concentrated along the internuclear axis and "π" represents orbitals that have no density on the internuclear axis. Traditionally, CO adsorption on clean transition-metal surfaces is considered to be largely determined by the donation of CO 5σ electrons to the substrate and back donation from the metal into the unoccupied $2\pi^*$ orbitals of CO (see, e.g., Ref. 39); the *quantitative* behavior of CO bonding to metal surfaces is more involved where the interaction and hybridization of the other orbitals (i.e., 4σ and 1π) with the metals states occur as well.[7,46–48] Recent experimental and theoretical studies have provided a considerably refined view of the CO metal bond and associated energetic contributions, as well as its dependence on adsorption site.[47,48] From the difference electron density distributions in Fig. 3, it can be seen that there is a depletion of electron density from the CO 5σ orbitals and an increase in the $2\pi^*$ states. For adsorption of CO in the on-top site, similar features occur for each system. For CO in hollow sites (see rightmost plot in Fig. 3), in comparison, there is a larger depletion of the CO 5σ orbitals and a larger increase of electron density into the CO $2\pi^*$ orbitals. Also, the region of maximum electron density increase between CO and the metal surface (region of bond formation) occurs between the CO $2\pi^*$ orbitals and the Ru $4d$ orbitals that point out of the surface, rather than in the region directly between the CO molecule and on top of the Ru atom, as is the case for the on-top site adsorption. Furthermore, we see clearly the significant role of the metal d states of the Ru atoms to which CO binds, where in all cases they are depleted of electron density.

The atom-projected CO DOS are shown in the bottom panels of Fig. 3. For CO in the top site (dashed curve for $1O_h+2CO_{t,f}$) the results are similar for all of the systems shown here: The two lowest-lying states are largely CO 3σ- and 4σ-like, respectively. The next lowest-lying feature is due to two states: the CO 5σ state at a slightly lower energy—that is, hybridized with the metal $4d$ states—and the CO 1π-like state. With respect to free CO, this latter ordering is *reversed* in that on adsorption on the surface, the CO 5σ orbital lies below the 1π level whereas in free CO it is the highest occupied molecular orbital (see upper curve of Fig. 6). There is also occupation of the CO $2\pi^*$ orbital as seen below the Fermi level. The molecular states most affected by interaction with the substrate are the 5σ and $2\pi^*$. With respect to hollow site adsorption of CO, the projected DOS exhibits the following general differences to on-top site adsorption: The CO 3σ-level is higher in energy and the 4σ lower in energy; furthermore, there is a hybridization of the 1π-like state due to interaction of the adparticles, seen, in particular, for CO in the $3O_h+1CO_h$ structure where the distances between adparticles are the smallest (shown in more detail in Fig. 2, as discussed above).

V. ENERGY BARRIERS FOR CO ADSORPTION

We now turn to another aspect of these systems: namely, the possibility of kinetic hindering to CO adsorption due to the presence of energy barriers. For the structures shown in Fig. 3, we have calculated the total energy as a function of the height of the carbon atom of the CO molecule above its adsorption site. The atomic positions of all other atoms are fully relaxed at each step, except that we (initially) constrain the CO axis to be perpendicular to the surface (with the C end towards the surface) and that the bottom two Ru layers of the slab are held fixed. The results are shown in Fig. 4 (solid circles).

For the $1O_h+1CO_t$ phase, the results show direct, unactivated adsorption of CO into the on-top site. This is consistent with experiments which measure a high sticking coefficient for CO coverages $\leqslant 1/4$. Also showing unactivated

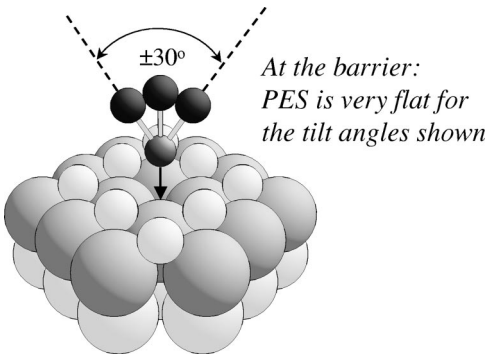

FIG. 5. Atomic geometry at the CO adsorption barrier maximum for the $3O_h+1CO_h$ structure, indicating that the potential energy surface (PES) is very flat with respect to tilt angles of the CO axis: For tilts of ±30° to the surface normal, the energy changes by less than 0.05 eV. Large and small pale circles represent Ru and O atoms, respectively, and dark circles CO. Note that for the CO molecule, the two additional O atoms shown are intended just to help indicate the tilts of the CO axis.

adsorption is the result for the $2O_{h,f}+1CO_t$ phase. On adding a second CO molecule into the fcc site of the $1O_h+1CO_t$ phase to form the $1O_h+2CO_{t,f}$ structure, an activation barrier of ≈0.2 eV is found. Interestingly, it can be seen that there is also a physisorption well of ≈0.1 eV at about 2.5 Å from the surface. We note that the employed exchange-correlation functional does not describe the long-range van der Waals interactions, so the depth of the physisorption well may not be accurate. Experimentally, in order to achieve adsorption of CO into the fcc site, higher CO exposures are required,[25] i.e., $\approx 10^5$ langmuir (L) ($1\,L=10^{-6}$ Torr s). In correspondence, the sticking coefficient, which is initially close to 1, drops by a factor of 60 at CO coverages greater than about 0.25. Thus, our calculated energy barrier, together with the decrease in available adsorption sites, is consistent with, and helps explain, the experimentally reported drop in sticking coefficient. The adsorption of CO into the vacant hcp site of the (2×2)-$3O_h$/Ru (0001) structure (which exists in nature[49,50]) also exhibits an energy barrier, in this case of ≈0.35 eV. This implies that CO pressures higher than those used to obtain the $1O_h+2CO_{t,f}$ structure mentioned above would be required in order to realize this structure experimentally.

We explored whether or not releasing the constraint that the CO axis be held perpendicular to the surface would yield a reduction of the identified energy barriers. We tested all possible directions and found that the barriers remain, and are in fact smallest for the assumed collinear geometry—the potential energy surfaces are, however, found to be very flat for a range of angles. In particular, for the $3O_h+1CO_h$ system, tilts of up to ±30° away from the surface normal in any azimuth yield an increase in the energy barrier of less than 0.05 eV. For larger angles the energy barrier becomes larger. This is depicted in Fig. 5. For the $1O_h+2CO_{t,f}$ structure, the PES is even flatter, with larger angles of up to ±41° not changing the barrier height by more than 0.03 eV for tilts towards neighboring O atoms. For tilts towards neighboring CO atoms, the angle is smaller for the same energy deviation: namely, ±36°. These larger angles can be understood in that for this structure, the neighboring adparticles are farther away and the repulsion slightly less.

To gain insight into the mechanisms responsible for the buildup of the energy barriers, we first consider the work-function change with respect to the underlying structure versus distance of CO from its equilibrium position on the surface (open circles in Fig. 4). It can be seen that in *all* cases considered there is a strong minimum present for CO at about 1.0 Å above its equilibrium position and then an abrupt increase occurs. We also show the difference density $n^{\Delta}(\mathbf{r})$ of the coadsorption system with CO at 1 Å above its equilibrium position, where the barriers are a maximum (when present) and where the work-function change is a minimum (see middle panels of Fig. 4). For no energy barrier, in both cases (two leftmost figures) charge has been depleted from the Ru $4d_{z^2}$ states and accumulation has occurred in the bonding region between the Ru and C atoms, and also into the Ru $4d_{xz,yz}$ states. We can also notice a redistribution of charge in the molecule; i.e., electron density is depleted from the 5σ-like orbitals and there is a slight enhancement in the $2\pi^*$-like states. These changes can be observed already for CO at larger distances, i.e., between 1.5 and 2.0 Å above the surface (i.e., distances of the C atom of CO from its equilibrium position) as we found from analysis of the (relative) number of electrons in the atomic orbitals as a function of distance. With closer distances of CO to the surface, the bonding charge between C and Ru increases and back donation into the CO $2\pi^*$ orbitals occurs (see Fig. 3), therefore strengthening and forming the Ru-CO bond. Concomitant with this movement of the electron density into these regions is the rather sudden increase in the work function, which sets in as soon as the wave functions start to significantly overlap. It is interesting to note that the ''action of bonding'' takes place ''quickly,'' i.e., over a short and critical distance: The adsorption energy increases by 1.08 eV and 1.07 eV over a distance of just 0.5 Å, respectively, for the $1O_h+1CO_t$ and $2O_{h,f}+1CO_t$ structures.

For the case of an energy barrier to CO adsorption, in both situations (two rightmost figures of Fig. 4), the electron density redistribution in the surface region appears *opposite* to when there is no barrier: There is *enhancement* into the Ru $4d$ states (and the O $2p_z$ orbitals for the $3O_h+1CO_h$ structure) and charge *depletion* from the region on the surface directly below the molecule, and no increase in electron density in the bonding region between CO and Ru. There is also depletion from the CO 5σ orbital and an increase in the $2\pi^*$-like states. Similarly, these redistributions begin to take effect already at about 1.5–2.0 Å above the surface. To try and understand the origin of the energy barrier and of the weak physisorption well, we analyzed the DOS and difference density for the $1O_h+2CO_{t,f}$ structure for different distances of the CO molecule from the surface: namely, 6 Å (CO far from the surface), 2.5 Å (corresponding to the physisorption well minimum), 1 Å (corresponding to the barrier maximum), and in its equilibrium position. The results are shown in Fig. 6. From the upper panel (left) of the difference density (CO at 6 Å), there is practically no interaction between CO and the surface. The corresponding DOS (upper-

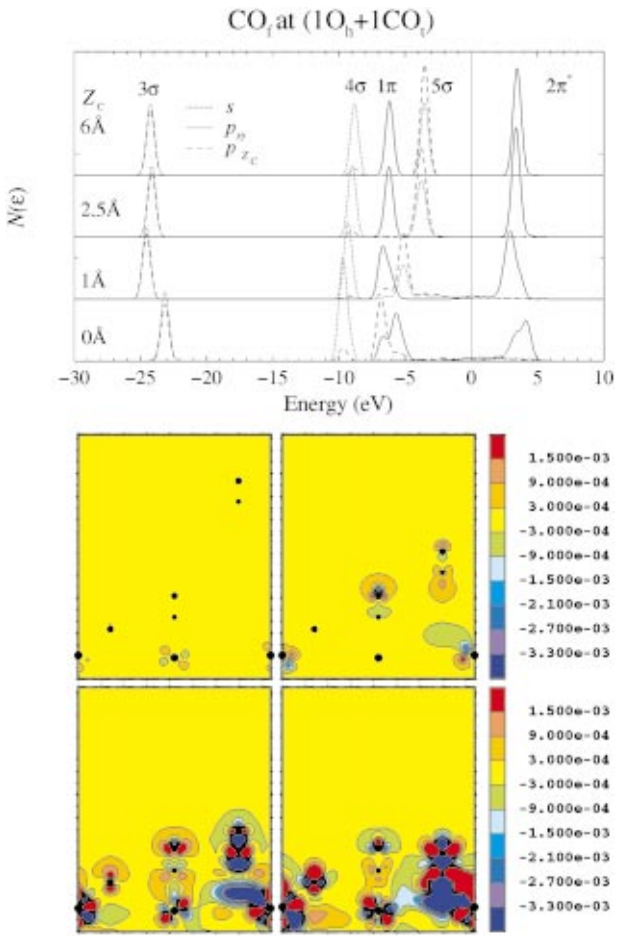

FIG. 6. (Color) Upper figures: projected DOS of the C atom of CO_f for different distances Z_C of CO_f above its fcc equilibrium site of the $1O_h+2CO_{t,f}$ structure. Lower figures: corresponding difference density, $n^{\Delta}(\mathbf{r})$, plots for CO_f at 6 Å (upper left), at 2.5 Å, corresponding to the weak physisorption well (upper right), 1 Å at the barrier maximum (lower left), and in its equilibrium position (lower right). The units are in e bohr^{-3}. Note the contour lines are a factor of ten smaller than those in Fig. 3.

most curve in Fig. 6) are essentially those of the free CO orbitals, but aligned with the substrate Fermi level: namely, 3σ, 4σ, 1π, 5σ, and the unoccupied $2\pi^*$ state (in order of lowest to highest energy).

At the physisorption well [upper right $n^{\Delta}(\mathbf{r})$ plot in Fig. 6], we can see that CO is ''polarized'' with an electron density increase at the C atom. There is also a polarization of the adsorbed CO_t molecule, with an increase in electron density at the O end of the CO_t molecule, i.e., towards the incoming CO_f molecule. On plotting $n^{\Delta}(\mathbf{r})$ on a smaller scale, an increase in electron density can clearly be seen connecting the C atom of CO_f and the O atom of CO_t. Furthermore, a depletion of the electron density at the adsorption site on the surface can be noticed which is related to Ru $d_{xz,yz}$-like states (with some extended *s*-like character). The distance between the C and O atoms (i.e., the C atom of the incoming CO_f and the O atom of the adsorbed CO_t) is 3.36 Å—notably longer than the CO bond length (e.g., 1.16–1.20 Å, cf. Table I). This distance is *very similar* to that which we found for our investigation into CO oxidation via an Eley-Rideal reaction, where a physisorption well for the C atom of CO at 3.5 Å directly above the adsorbed O atom [i.e., the distance between C and O(ad)] was found.[51] This suggests that the mechanism giving rise to both these wells may have the same origin, which the above analysis shows is due to an attractive overlap of the *tails* of the wave functions associated with the above-mentioned particles. The DOS at the physisorption well minimum exhibits only slight changes as compared to when CO is far from the surface, e.g., a small upward shift in the CO_f 3σ and an equally small downward shift of the CO_f 5σ orbitals, which is consistent with the increase in electron density at the C atom of CO_f and of the slight increase in adsorption energy, respectively.

At closer distances to the surface—namely, at the barrier maximum, 1 Å from the surface—the wave functions begin to overlap. The electron density is further displaced *away* from the region on the surface directly beneath the CO molecule and into Ru $4d_{z^2}$ states and, in contrast to at the well minimum, also out of the CO 5σ orbitals. There is enhancement of the electron density into the CO $2\pi^*$ states and also into the adsorbed CO_t molecule and the O_h adatom. (Note that this was shown already in Fig. 4, but plotted on a different scale.) The observed displacement of the electron density away from the bonding region of these entities (CO_f and surface with preadsorbed CO_t and O_h) indicates a *repulsive* interaction. At this position of CO_f from the surface, the DOS show that the CO 3σ orbital moves to a slightly lower energy as does the 4σ. The 5σ state is notably lower in energy and *broadened* compared to when CO_f is at 2.5 Å. The development of some higher-lying states of *s* and p_z character (i.e., CO 5σ-like) in the region -4 to -2 eV can be noticed. These states are identified as being antibonding-like through investigating the spatial distributions of the wave functions. That is, the sign of the involved (approaching) CO 5σ-like wave function is *opposite* to those that it interacts with at the surface. The development of such antibondinglike states is largely responsible for the repulsive (Pauli-like) interaction[52] and the energy barrier.

With even closer distance of CO_f to the surface, i.e., at the equilibrium geometry, a significant increase of the electron density into the CO $2\pi^*$ states occurs, which form a bond involving the Ru $4d_{z^2}$ orbitals. This can be clearly seen in the lower right $n^{\Delta}(\mathbf{r})$ plot of Fig. 6. The corresponding DOS also show significant changes, in particular that the CO 5σ-like state has moved down in energy to below the CO 1π state and the CO 3σ state up in energy. The 1π-derived orbital also exhibits a broadening and hybridization due to interaction with O-Ru states, in which the O atoms bond to the same Ru atoms as CO_f.

The described electron redistribution, or polarization, of the CO molecules taking place at the physisorption well minimum of the $1O_h+2CO_{t,f}$ structure also explains the weak maxima seen in the work-function change at this distance (see Fig. 4); i.e., an induced effective surface dipole moment that points towards the surface—i.e., the negative end outside the surface [as is the case in the upper right $n^{\Delta}(\mathbf{r})$ plot of Fig. 6]—will give rise to an increase in the work function, as observed. At closer distances to the sur-

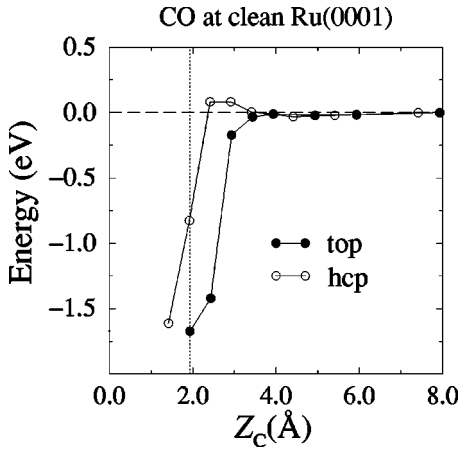

FIG. 7. Total energy, referred to the situation where CO is far from the surface, for CO above the top (solid circles) and hcp hollow (open circles) sites of the clean Ru(0001) surface with the CO axis perpendicular to the surface and the C end down, as a function of distance of CO from the position of the Ru atom(s) to which the C atom binds.

face, the above-mentioned repulsive interaction becomes dominant and displaces the electron density away from the adsorption site into the Ru states as seen in the $n^{\Delta}(\mathbf{r})$ distributions (Figs. 4 or 6) and also out of the CO 5σ state. The maximum of this repulsion coincides with the observed decrease and minimum in the work function. At even closer distances, bond formation involving the CO $2\pi^*$ states and the Ru $4d_{z^2}$ states that point out of the surface can occur, thus giving rise to an increase in the electron density in the bonding region and in the $2\pi^*$ states (see, e.g., the difference density in far right panel of Fig. 3) and therefore the corresponding abrupt increase in the work function, as the bond formation is completed.

Finally, we considered the possibility of the existence of energy barriers to adsorption of CO at the *clean* Ru(0001) surface. In Fig. 7 we show the total energy versus distance of CO from the surface, above the top and hcp hollow sites. As before, the CO axis is held perpendicular to the surface with the C end down and atomic relaxation included at every step. For the top site, no energy barrier occurs, as was the case for the coadsorption systems where CO adsorbed in on-top sites. For CO at the hcp site, however, we observe a small barrier of 0.08 eV. The energetics in Fig. 7 show that CO from the gas phase will be initially attracted to top sites, which is the most stable site for adsorption on Ru(0001). In each case (top and hollow) the work-function change as a function of distance exhibits a similar behavior as shown earlier for the coadsorption systems, namely, a minimum at about 1 Å for the C atom of CO above its equilibrium position, and a sharp increase for closer distances as the molecule-substrate wave functions start to overlap and form the bond.

It is interesting to consider the mechanism giving rise to the barrier in this case as there are no coadsorbates present. In order to gain insight into this, we calculated the difference density distributions for CO at the hcp site at 1 Å above the surface. The obtained electron redistribution taking place in the CO molecule and at the surface Ru atoms is found to be very similar to that described above for the $1O_h+2CO_{t,f}$ system (Fig. 6, lower left), the barrier being larger in the latter case because the displacement of charge out of the surface Ru $4d_{xz,yz}$ states and into the Ru $4d_{z^2}$ states also disturbs and destabilizes the binding of the preadsorbed (CO_t and O_h) adparticles.

The found presence of activation barriers for nondissociative adsorption carries with it some possible implications for the interpretation and modeling of experimental results and theoretical simulations of surface processes. For example, with respect to the former, we may think of thermal desorption which is one of the most widely used experimental techniques for studying the binding energies of adsorbed species. In this experiment one prepares an adsorbate layer of a given initial coverage at a given temperature and measures the desorption rate of the particular species as a function of increasing temperature. From such experiments the desorption energy can be determined, i.e., the energy needed to remove a particle from the surface and bring it into the gas phase. Often this value is directly correlated with the binding energy of the adparticle to the surface, and if there is an activation barrier for adsorption, it would imply that the binding energy would be *overestimated* by the barrier height, given that the binding energy is typically referred to the energy of the particle in the gas phase (away from the surface). Concerning theoretical simulations of experimental data, using, e.g., kinetic rate equations or *ab initio* calculations of surface processes using kinetic Monte Carlo calculations, the effect of the neglect of such activation barriers to adsorption could have consequences for the results and their interpretation; e.g., if, as is often done, the coverage of a species on the surface is assumed to be directly related to the deposition rate (which may be reasonable for low coverages), but if in reality barriers are present, the resulting coverage will be less than assumed from the applied deposition rate. For example, the found activation barriers for CO adsorption of 0.2 and 0.35 eV (assuming a simple Arrhenius relationship and room temperature) will yield factors of 4.4×10^{-4} and 1.3×10^{-6} less for the number of particles hitting the surface, respectively, which is considerable.

VI. CONCLUSION

In summary, we have investigated the energetics and interactions of (2×2)-$(n\mathrm{O}+m\mathrm{CO})$/Ru (0001) coadsorption systems. We observed behavior consistent with the general picture that increasing the O coverage results in a decrease of the CO binding energy. This occurs when CO occupies a hollow site and O atoms bond to the *same* Ru atoms as CO. We also find behavior different to this: namely, that with an increase in O coverage there can be practically no change or even a slight *increase* in the CO adsorption energy. This occurs for CO in the top site, and we attribute the slight increase in energy as being due to an O-induced lateral weakening of Ru-Ru bonds that reduces the ''effective coordination'' and destabilizes the non-O-bonded Ru atom that CO bonds to making it more reactive, thus binding the CO molecule more strongly. This destabilization is quantified by a significant reduction in the energy required to remove the nonbonded Ru atom of as much as 1.4 eV. Thus, a decrease

in the CO adsorption energy is primarily expected with an increase in the number of O atoms that *share a bond with the same Ru atoms to which CO is bonded*, not simply with the O coverage *per se*. Analogous calculations involving the coadsorption of CO and the electropositive atom Na, instead of the electronegative atom O, show a qualitatively *opposite* behavior. We also identified the presence of activation barriers for CO adsorption, which are preceded by a weak physisorption well. The origin of the latter is attributed to an attractive interaction between the *tails* of the wave functions of the preadsorbed species and the approaching CO molecule, while the origin of the former is attributed to a Pauli-like repulsive interaction involving occupation of weak antibondinglike states. We anticipate that the identified mechanisms and behavior may also be valid for other similar systems.

[1] *The Chemical Physics of Solid Surfaces and Heterogeneous Catalysis*, edited by D. A. King and D. P. Woodruff (Elsevier, New York, 1982), Vol. 4.

[2] G. Ertl, Surf. Sci. **299-300**, 742 (1994); *Handbook of Heterogeneous Catalysis*, edited by G. Ertl, H. Knözinger, and J. Weitkamp (Wiley, New York, 1997).

[3] D.W. Goodman, Surf. Sci. **299-300**, 837 (1994).

[4] G.A. Somorjai, Surf. Sci. **299-300**, 849 (1994); *Introduction to Surface Chemistry and Catalysis* (Wiley, New York, 1994).

[5] MRS Bull. **24**, No. 7 (1999). See, especially pp. 12, 16, 24, 29, and 43.

[6] MRS Bull. **24**, No. 6 (1999). See, especially pp. 14, 18, 25, 44, and 49.

[7] M. Scheffler and C. Stampfl, in *Electronic Structure, Handbook of Surface Science*, Vol. 2, edited by K. Horn and M. Scheffler (Elsevier, Amsterdam, 2000), p. 286.

[8] T. Engel and G. Ertl, Adv. Catal. **28**, 1 (1979).

[9] F.M. Hoffmann, M.D. Weisel, and C.H.F. Peden, Surf. Sci. **253**, 59 (1991).

[10] C. H. F. Peden, in *Surface Science of Catalysis: In situ probes and reaction kinetics*, edited by D. J. Dwyer and F. M. Hoffmann (American Chemical Society, Washington, DC, 1992).

[11] A. Böttcher, H. Niehus, S. Schwegmann, H. Over, and G. Ertl, J. Phys. Chem. **101**, 11 185 (1997).

[12] A. Böttcher and H. Niehus, Phys. Status Solidi A **173**, 101 (1999).

[13] A. Böttcher, B. Krenzer, H. Conrad, and H. Niehus, Surf. Sci. Lett. **466**, L811 (2000).

[14] H. Over, Y.D. Kim, A.P. Seitsonen, S. Wendt, E. Lundgren, M. Schmid, P. Varga, A. Morgante, and G. Ertl, Science **287**, 1474 (2000).

[15] C. Stampfl and M. Scheffler, Phys. Rev. B **54**, 2868 (1996); C. Stampfl, Surf. Rev. Lett. **3**, 1567 (1996).

[16] C. Stampfl, S. Schwegmann, H. Over, M. Scheffler, and G. Ertl, Phys. Rev. Lett. **77**, 3371 (1997).

[17] C. Stampfl and M. Scheffler, Phys. Rev. Lett. **78**, 1500 (1997).

[18] C. Stampfl, H.J. Kreuzer, S.H. Payne, and M. Scheffler, Appl. Phys. A: Mater. Sci. Process. **69**, 471 (1999).

[19] K. Reuter, C. Stampfl, M. V. Gandgulia-Pirovano, and M. Scheffler, Chem. Phys. Lett. **352**, 311 (2002).

[20] K. Reuter, M. V. Gandgulia-Pirovano, C. Stampfl, and M. Scheffler, Phys. Rev. B **65**, 165403 (2002).

[21] C. Stampfl, M. V. Ganduglia-Pirovano, K. Reuter, and M. Scheffler, Surf. Sci. **500** (to be published).

[22] K.L. Kostov, H. Rauscher, and D. Menzel, Surf. Sci. **278**, 62 (1992).

[23] B. Narloch, G. Held, and D. Menzel, Surf. Sci. **340**, 159 (1995).

[24] B. Narloch, G. Held, and D. Menzel, Surf. Sci. **317**, 131 (1994).

[25] A. Schiffer, P. Jakob, and D. Menzel, Surf. Sci. **389**, 116 (1997).

[26] C. Stampfl and M. Scheffler, Isr. J. Chem. **38**, 409 (1998).

[27] M. Kiskinova, Surf. Sci. Rep. **8**, 399 (1988).

[28] J. K. Nørskov, in *The Chemical Physics of Solid Surfaces, Coadsorption, Promoters and Poisons*, edited by D. A. King and D. P. Woodruff (Elsevier, Amsterdam, 1993), Vol. 6.

[29] N. Troullier and J.L. Martins, Phys. Rev. B **43**, 1993 (1991).

[30] M. Fuchs and M. Scheffler, Comput. Phys. Commun. **119**, 67 (1999).

[31] R. Stumpf and M. Scheffler, Comput. Phys. Commun. **79**, 447 (1994); M. Bockstedte, A. Kley, J. Neugebauer, and M. Scheffler, *ibid.* **107**, 187 (1997).

[32] J.P. Perdew, J.A. Chevary, S.H. Vosko, K.A. Jackson, M.R. Pederson, D.J. Singh, and C. Fiolhais, Phys. Rev. B **46**, 6671 (1992).

[33] S.L. Cunningham, Phys. Rev. B **10**, 4988 (1974).

[34] H.J. Monkhorst and J.D. Pack, Phys. Rev. B **13**, 5188 (1976).

[35] H. Pfnür and D. Menzel, J. Chem. Phys. **79**, 2400 (1983).

[36] G. Michalk, W. Moritz, H. Pfnür, and D. Menzel, Surf. Sci. **129**, 92 (1983).

[37] H. Over, W. Moritz, and G. Ertl, Phys. Rev. Lett. **70**, 315 (1993).

[38] P.J. Feibelman, B. Hammer, J.K. Nørskov, F. Wagner, M. Scheffler, R. Stumpf, R. Watwe, and J. Dumesic, J. Phys. Chem. **105**, 4018 (2001).

[39] G. Blyholder, J. Phys. Chem. **68**, 2772 (1964).

[40] M. Mavrikakis, B. Hammer, and J.K. Nørskov, Phys. Rev. Lett. **81**, 2819 (1998).

[41] B. Hammer, Phys. Rev. B **63**, 205423 (2001).

[42] C.J. Zhang, P. Hu, and M.-H. Lee, Surf. Sci. **432**, 305 (1999).

[43] W.-X. Li, C. Stampfl, and M. Scheffler, Phys. Rev. B **65**, 075407 (2002).

[44] M. Schmid, G. Leonardelli, M. Sporn, E. Platzgummer, W. Hebenstreit, M. Pinczolits, and P. Varga, Phys. Rev. Lett. **82**, 355 (1999).

[45] A. Eichler and J. Hafner, Phys. Rev. B **62**, 5163 (2000).

[46] P. Hu, D.A. King, M.-H. Lee, and M.C. Payne, Chem. Phys. Lett. **79**, 4613 (1996).

[47] A. Föhlisch, M. Nyberg, J. Hasselström, O. Karis, L.G.M. Pettersson, and A. Nilsson, Phys. Rev. Lett. **85**, 3309 (2000).

[48] A. Föhlisch, M. Nyberg, P. Bennich, L. Triguero, J. Hasselström, O. Karis, L.G.M. Pettersson, and A. Nilsson, J. Chem. Phys. **112**, 1946 (2000).

[49] Y.D. Kim, S. Wendt, S. Schwegmann, H. Over, and G. Ertl, Surf. Sci. **418**, 267 (1998).

[50] M. Gsell, M. Stichler, P. Jakob, and D. Menzel, Isr. J. Chem. **38**, 339 (1998).

[51] C. Stampfl, H.J. Kreuzer, S.H. Payne, H. Pfnür, and M. Scheffler, Phys. Rev. Lett. **83**, 2993 (1999).

[52] R. Hoffmann, *Solids and Surfaces: A Chemist's View of Bonding in Extended Structures* (VHC Verlag, Weinheim, Germany, 1988).